

# Structural Integrity of Fuselage Panels with Multisite Damage

Jai H. Park,\* Ripudaman Singh,† Chang R. Pyo,‡ and Satya N. Atluri§  
*Georgia Institute of Technology, Atlanta, Georgia 30332*

**S**tructural integrity assessment of aging flight vehicles is extremely important to ensure their economic and safe operation. A two-step analytical approach, developed to estimate the residual strength of pressurized fuselage stiffened shell panels with multi-bay fatigue cracking is presented in this article. Conventional finite element analysis of the damaged multibay panel is first carried out to obtain the load flow pattern through it. The Schwartz-Neumann alternating method is then applied to the fuselage skin with multiple site damage, to obtain stresses and the relevant crack tip parameters that govern the onset of fracture. Fracture mechanics as well as net section yield criteria are used to evaluate the static residual strength. The presence of holes with or without multisite damage ahead of a dominant crack is found to significantly degrade the capacity of the fuselage shell panels to sustain static internal pressure. An elastic-plastic alternating method is newly developed and applied to evaluate the residual strength of flat panels with multiple cracks. The computational methodologies presented herein are marked improvements to the present state-of-the-art, and are extremely efficient, both from engineering manpower as well as computational costs point of view. Once verified, they can very well complement the experimental requirements, reducing the cost of structural integrity assessment programs.

## Introduction

**R**ESIDUAL strength estimations of critical components of in-service aircraft that have exceeded their initial design life are imperative for their safe operation. This article presents a part of the major effort being made to develop reliable computational tools for structural integrity evaluation of aging as well as new airplanes. These computational tools are envisioned to involve the least amounts of engineering man power as well as computer resources.

The microcracks emanating at material/structure imperfections grow under static and fatigue loading and coalesce to form detectable cracks. In order to ensure safety, it is important to understand the severity of these cracks and also to have an estimate of the collapse strength of the damaged structure. This article primarily deals with the investigation of longitudinal cracks in stiffened fuselage shell panels. In an airliner fuselage, pressurization causes stresses in the shell structure. The stiffeners (stringers, frames, and tear straps) take a part of the load, but the major fraction is taken by the skin. Large cracks in the skin cause significant redistribution of load flow that becomes fairly complex due to various stiffening elements and the presence of holes/multisite damage (MSD) ahead of a dominant crack. Thus, the problem essentially calls for a determination of the load flow pattern through the panel, before the crack tip stresses and other relevant crack tip parameters such as the stress intensity factor (SIF),  $T^*$ , etc., that govern the onset of fracture, can be determined.

Conventional finite element analysis of the multibay shell panel with cracks generates information about the realistic load flow pattern through the panel. The cracked portion of the shell is then isolated with the corresponding sheet stresses and the fastener loads (if any). The finite element alternating

method has been found to provide good quantitative estimates of crack tip fracture parameters.<sup>1</sup> This sequential combination of two-step finite element methods (FEM) forms an efficient computational tool for the estimation of static residual strength. For materials with significant ductility, an elastic plastic alternating method has been developed by Nikishkov and Atluri,<sup>2</sup> which generates a very accurate elastic-plastic stress state solution near the crack tips by using only the finite element model of the uncracked sheet. This technique has been extended to study the MSD in Al 2024-T3 skin in the present article. In both techniques<sup>1,2</sup> the use of a single finite element mesh is adequate to study a variety of cracks, of varying lengths, in the skin. This makes the present analysis extremely efficient.

## Problem Definition

Consider a fuselage shell panel of radius 118.5 in. and thickness 0.071 in. made out of aluminium Al 2024-T3. This shell is stiffened longitudinally by frames (Al 2024-T3) spaced at 20 in., with 0.7171 in.<sup>2</sup> and 1.432 in.<sup>4</sup> of cross-sectional area and moment of inertia, and placed inside of the shell with their neutral axis at 3.25 in. from the shell midplane. At all frame locations there are Ti 8-1-1 tear-straps 3 × 0.025 in. Circumferentially, the shell is stiffened by stringers (Al 2024-T3) spaced at 8 in., with 0.6721 in.<sup>2</sup> and 0.102 in.<sup>4</sup> of area and moment of inertia, and placed inside of the shell with their neutral axis at 0.68 in. from the shell midplane. The frames and the stringers are attached to the skin by a row of

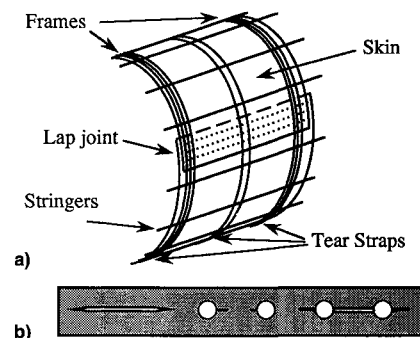


Fig. 1 Fuselage shell panel configuration: a) shell panel and b) cracked skin segment.

Received July 19, 1993; revision received July 30, 1994; accepted for publication Sept. 1, 1994. Copyright © 1994 by the American Institute of Aeronautics and Astronautics, Inc. All rights reserved.

\*Visiting Scholar; currently FAA Center of Excellence for Computational Modeling of Aircraft Structures, Chungbuk National University, Cheongju, Republic of Korea.

†Postdoctoral Fellow, FAA Center of Excellence for Computational Modeling of Aircraft Structures. Member AIAA.

‡Postdoctoral Fellow, FAA Center of Excellence for Computational Modeling of Aircraft Structures.

§Institute Professor and Regents' Professor of Engineering, FAA Center of Excellence for Computational Modeling of Aircraft Structures. Fellow AIAA.

fasteners, 0.1875 in. in diam placed at a pitch of 1.25 in. The fuselage is subjected to an internal pressure of 8.6 psi.

For the longitudinal lap joint in the panel, consider a configuration of three rows of 0.15625-in. Al rivets at 1 in. pitch and a total of 3 in. overlap. At the lap there is a layer of adhesive 0.0065 in. thick with  $G_a = 1.09 \times 10^5$  psi.

The material properties of Al 2024-T3 are taken as  $E = 10.5 \times 10^3$  ksi,  $\nu = 0.32$ ,  $\sigma_y = 47.0$  ksi,  $\sigma_u = 64.0$  ksi, crack tip link-up stress  $\sigma_{lu} = \frac{1}{2}(\sigma_y + \sigma_u) = 55.5$  ksi, and fracture toughness  $K_c = 93.0$  ksi- $\sqrt{\text{in.}}$ . The above-mentioned details are realistic to the best of the authors' knowledge, in the absence of the exact data from the industry. Three situations of cracks are considered in this article: 1) a dominant multibay crack, 2) a dominant multibay crack at a row of fastener holes, and 3) a dominant multibay crack with/without MSD at the lap splice.

In addition, a full elastic-plastic analysis of a flat panel with multiple cracks is performed, the configurational details of which are given separately in the corresponding section.

### Analytical Approach

The method of analysis adopted is to first evaluate the load flow through the damaged panel and then perform a refined analysis to obtain stress fields at the various crack tips. Global-local finite element analysis procedure has been developed for this purpose.

#### Global Analysis (FEM)

Conventional linear elastic finite element analysis of the multibay stiffened shell panel with cracks is performed as a part of the global analysis. The FEM model is briefly described below:

The fuselage skin and the tear straps are modeled by four-noded shell elements with 5 degrees of freedom (DOF) per node.<sup>3</sup> The frames and stringers are modeled as two-noded, curved/straight beam elements compatible with the sheet. The cracks are incorporated into the problem as unconnected nodes belonging to respective elements. For the purpose of present global analysis, the crack tip singularity is not modeled because the crack will be modeled analytically in the second step, i.e., the local analysis. The fasteners and the adhesive are modeled as 2 degree-of-freedom connectors between the corresponding nodes.<sup>4,5</sup> Appropriate multipoint-constraints are imposed to prevent criss-crossing of sheet nodes in the lap joint zone. The fuselage internal pressure is applied as a uniformly distributed normal outward load on the shell panel. The four edges of the panel are permitted to undergo only a radial displacement in the cylindrical system. A typical problem size would consist of about six bays in each direction because it is expected that the effect of damage would fully die out about two bays away on each side of the damaged bay. For these configurations, the size of the finite element model is of the order of 15,000 DOF and the computer time is of the order of minutes on an HP 9000/700 series workstation.

#### Elastic Local Analysis (E-FEAM)

From the global analysis, the skin segment containing the cracks, holes, and fasteners of interest is isolated with corresponding sheet stresses. The fastener holes are now modeled as circular, and the bearing loads (if any from global analysis) are distributed as sinusoidal variations over the periphery. The stresses due to the misfit of the rivet can also be accounted for at this stage. This problem is solved using Schwartz-Neumann finite element alternating method (FEAM), which involves two solutions:

1) An analytical solution to the problem of a row of cracks of arbitrary lengths with crack faces being subjected to arbitrary tractions.

2) Finite element solution for a strip, with/without a row of holes, but without cracks; the strip being subjected to sheet

stresses and pin bearing loads. Since the finite element solution is only for the uncracked body, and the cracks of arbitrary lengths are accounted for analytically in step 1 above, the computational finite element mesh remains the same as the cracks grow.

This technique and the analytical solution to the problem of multiple cracks in an infinite sheet are presented in detail in an earlier work by Park et al.<sup>5</sup> In this finite element analysis, eight-noded isoparametric elements with 2 DOF per node are employed.

The crack tip stress intensity factors and the stress field are obtained directly from the FEAM analysis. The net section stress for any ligament is obtained by taking an average over the ligament length. Critical pressure for the fuselage is that value of applied pressure differential for which either the crack tip SIF becomes equal to  $K_c$  of 93.0 ksi- $\sqrt{\text{in.}}$ , or the net ligament stress equals the link-up stress of 55.5 ksi. For linear elastic analysis, this can be computed directly from the obtained values of  $K_t$  and average ligament stress  $\sigma_{av}$ :

$$\text{critical pressure differential} = \text{applied pressure} \times (K_c/K_t)$$

$$\begin{aligned} \text{critical pressure differential} &= \text{applied pressure} \\ &\times (\text{linkup stress}/\sigma_{av}) \end{aligned}$$

There will be some out-of-plane bending associated with the sheet close to the crack. A FEAM for plate bending problems is under development and will be integrated with the total computational procedure shortly. A methodology has been developed for problems with significant bulging at the cracked edges and forms the subject matter of a separate presentation.<sup>6</sup>

#### Elastic-Plastic Local Analysis (EP-FEAM)

The elastic-plastic finite element alternating algorithm uses the elastic finite element alternating technique in conjunction with the initial stress method.<sup>7</sup> The solution of the cracked sheet problem is obtained by adding the influences of the plastic strain as artificial volume loads on an elastic body, the analytical solution for cracked infinite elastic medium, and the finite boundary corrections. The details of this algorithm are described in the paper by Nikishkov and Atluri,<sup>2</sup> and for the case of multiple cracks the concept of this algorithm is shown in Fig. 2. Since the singular stress field is obtained through the analytical solutions for the cracked infinite medium, this eliminates the need for a very fine mesh discretization around the crack tip.

The elastic-plastic alternating technique has earlier been used to evaluate residual strength of flat panels,<sup>8</sup> and has now been extended to analyze stably growing MSD cracks and their link-up in flat panels. Atluri<sup>9</sup> defines an integral  $T^*$  as a measure of the severity of conditions around a small region around the crack tip of size  $\epsilon$  (i.e., process zone). This  $T^*$  integral,<sup>9</sup> based on the equivalent domain integral (EDI) method,<sup>10</sup> is employed as the crack tip parameter governing the stable crack growth. Since this integral is obtainable from EP-FEAM, a coarse mesh is adequate for stable tearing analysis in an incremental fashion.

To model stable tearing, the load on the cracked panel is continuously increased, with integral  $T^*$  being evaluated at each load step, until it reaches a critical value. The crack is then grown by an incremental length  $\Delta a$ . After this crack extension, the external load is adjusted so that the integral again attains the critical value. In EP-FEAM, the crack extension is modeled by releasing the cohesive traction ahead of the crack tip, relinquishing the need for remeshing. The analysis is continued by extending the crack length in increments of  $\Delta a$  during each crack propagation step. In a conventional nodal release technique, a row of very fine mesh discretization is required along the line of crack propagation. However, in the present work, the singularities in the stresses

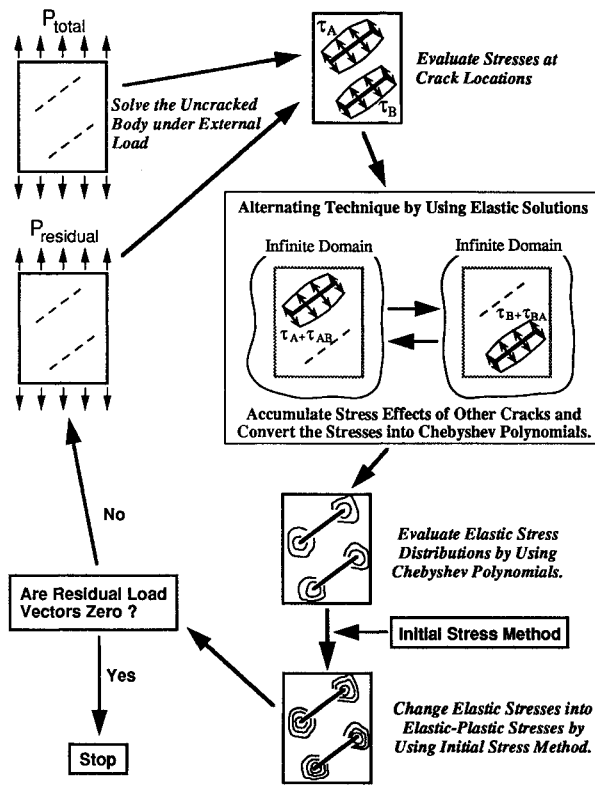


Fig. 2 Schematic of the elastic-plastic alternating method for multiple cracks.

and strains are accounted for by the use of the analytical solutions for a cracked infinite elastic medium. The algorithm utilizes two different analytical solutions. The first one is for a crack subjected to traction over the entire crack face. This is used when cracked body is initially loaded until the integral reaches a critical value and when the external loading is adjusted so that the value again becomes critical. The second one is for the traction at the face of the incremental portion of the crack, i.e.,  $\Delta a$  at both the ends of the crack. This analytical solution is used to release the cohesive traction ahead the crack tip during crack growth.

### Single Dominant Multibay Crack in the Skin

Consider the shell panel consisting of seven frames (six bays) and six stringers (five bays) with a single dominant crack aligned longitudinally and located centrally, i.e., halfway between two stringers and symmetrical about a frame/strap location. Swift<sup>11</sup> presents the requirement for the fuselage from the damage tolerance point of view. The fuselage stiffened shell must be able to sustain a two bay long crack with broken central strap. For this requirement, consider the central tear strap also to be cracked along with the skin. All other stiffening elements (including the frame at the location of broken strap) are intact.

Analyses have been carried out for various crack lengths up to 50 in., i.e., the crack spreading in four bays. Since there is only one crack and there are no holes in the vicinity of the crack tip, it is difficult to reasonably define an intact ligament length, thus the critical pressure is computed only from fracture mechanics point of view. This is shown in Fig. 3.

A point on this curve gives information about the cabin pressure required to make the crack tip SIF critical and does not imply that the panel will fail catastrophically. The curve falls below the applied pressure of 8.6 psi for crack lengths of 10.8 and 18.2 in.; points a and b. The implication of this is as follows. Considering an initial half-crack length of about 2 in., and the pressure never exceeding 8.6 psi, the crack cannot grow under static loading, it will grow under cyclic

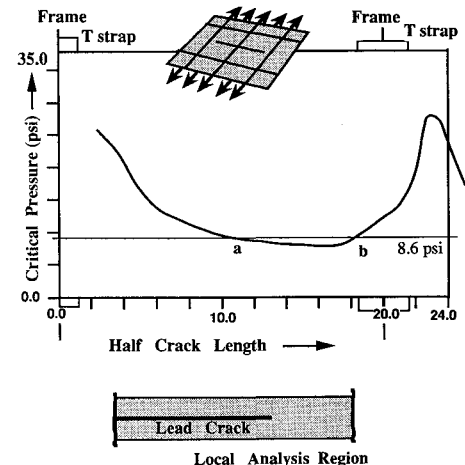


Fig. 3 Critical pressure diagram for a single dominant multibay crack in the shell panel.

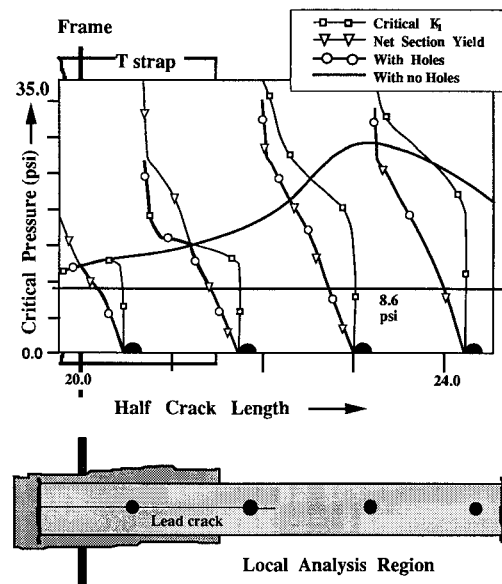


Fig. 4 Critical pressure diagram for a single dominant two-bay crack with holes ahead of the crack tip.

loading until it reaches point a. At this stage fast fracture will occur and the crack will instantaneously grow up to point b, where it will be arrested as the SIF falls below the critical value. Further growth of the crack will again be under cyclic loading. The effect of plasticity is not included in this calculation, and stable tearing that follows crack growth initiation is not modeled.

### Two-Bay Crack with Holes near the Crack Tip

Consider the same shell panel consisting of seven frames (six bays) and seven stringers (six bays) with a single dominant crack aligned longitudinally along the fastener holes. The crack is located centrally and is symmetrical about a frame/strap location. The central tear strap is broken. All other stiffening elements are intact. The presence of holes alters the stress flow. The distance between the crack tip and the hole periphery is found to have a substantial effect on the crack tip SIF, and also for very small ligaments the section will yield before the crack becomes unstable. A situation of holes ahead of a two-bay crack is analyzed to study the effect of holes on the critical pressure.

Figure 4 shows the effect of holes ahead of a two-bay crack. For the sake of convenience we will use a term overhang, defined as the extent of crack length from the closest hole

Table 1 Effect of MSD on  $K_I$ ,  $\sigma_{av}$ , and residual strength; set 1, constant MSD crack length of 0.12 in.

Half crack length	LEFM				Net section stress			
	$K_I$ , ksi- $\sqrt{\text{in.}}$		Critical pressure, psi		$\sigma_{av}$ , ksi		Critical pressure, psi	
	No MSD	MSD	No MSD	MSD	No MSD	MSD	No MSD	MSD
Lead crack overhang = 0.25 in.								
1.75	27.5	28.4	28.5	27.6	12.1	12.4	39.4	38.5
3.75	41.2	42.1	19.0	18.6	16.7	17.4	28.6	27.4
5.75	43.8	54.2	14.5	14.4	21.5	22.4	22.2	21.3
7.75	64.4	64.0	12.2	12.2	25.8	26.9	18.5	17.7
9.75	72.7	71.5	10.8	10.9	29.6	31.0	16.1	15.4
11.75	79.4	77.5	9.9	10.1	32.9	34.4	14.5	13.9
13.75	84.8	82.2	9.2	9.5	35.4	37.1	13.5	12.9
15.75	88.0	83.1	8.9	9.4	36.7	38.5	13.0	12.4
17.75	81.9	79.2	9.6	9.9	34.7	36.0	13.8	13.3
18.75	68.8	65.5	11.4	11.9	29.6	30.5	16.1	15.6
19.75	47.6	43.2	16.4	18.1	22.6	23.1	21.1	20.7
20.75	28.6	25.2	27.4	31.1	19.4	19.7	24.6	24.2
21.75	30.7	28.6	25.5	27.4	17.9	18.3	26.7	26.1
22.75	36.4	35.1	21.5	22.3	18.6	19.1	25.7	25.0
Lead crack overhang = 0.50 in.								
2.00	27.7	28.3	28.3	27.7	19.4	20.6	24.6	23.2
4.00	41.2	41.8	19.0	18.7	27.1	29.1	17.6	16.4
6.00	53.9	54.1	14.5	14.5	34.9	37.5	13.7	12.7
8.00	64.6	64.2	12.1	12.2	41.8	44.9	11.4	10.6
10.00	73.1	72.0	10.7	10.9	47.8	51.2	10.0	9.3
12.00	80.0	78.3	9.8	10.0	52.8	56.5	9.0	8.4
14.00	85.6	83.2	9.1	9.4	56.7	60.6	8.4	7.9
16.00	88.6	84.3	8.8	9.3	58.6	62.2	8.1	7.7
18.00	81.5	78.9	9.6	9.9	54.2	57.2	8.8	8.3
19.00	67.4	64.2	11.6	12.2	44.8	47.1	10.7	10.1
20.00	47.5	43.6	16.5	17.9	33.2	34.3	14.4	13.9
21.00	31.5	28.4	24.8	27.6	28.2	28.5	16.9	16.7
22.00	32.6	30.8	24.0	25.4	26.8	27.6	17.8	17.3
23.00	37.5	36.4	20.9	21.5	28.6	29.9	16.7	16.0

center involved in the same crack. Zero overhang implies a hole at the crack tip, and so the SIF has no definition. For extremely small overhang the SIF value is low, and for longer overhangs the SIF rises sharply. The ligament stress is found to increase steadily with overhang. For any crack length and overhang, the critical pressure is the lower of the two values corresponding to  $K_I = K_c$  and  $\sigma_{av} = \sigma_{tu}$ . Figure 4 shows the critical pressure from both the considerations, and interestingly, the structure is critical from net section failure point of view over most of the region. Again, any point on this curve represents the pressure differential required to either make the crack unstable or cause tensile failure of the ligament. It is seen from this analysis that the presence of holes (even without cracks emanating from them) ahead of a lead crack, significantly lowers the residual strength of a stiffened panel; as surmised by Swift.<sup>11,12</sup>

### Two-Bay Cracking at Lap Splice

We now consider the aspect of a multibay crack with and without an MSD ahead of it. In this section, we consider the shell panel consisting of six bays in longitudinal direction and six bays along the circumferential direction and a lap joint. Let there be a long crack extending equally on two sides of the central broken tear strap. Generally, the adhesive is found to degrade very fast,<sup>13</sup> and we consider a 99% degradation in adhesive shear strength for the present analysis. All the other stiffening elements (frames, tear straps, and stringers) are considered intact. We are interested in the residual strength for various lead crack lengths and the effect of MSD ahead of the crack tip.

#### Single Dominant Crack at Fastener Holes

First consider the situation of a single dominant crack only. Global analysis is carried out to obtain the rivet bearing loads

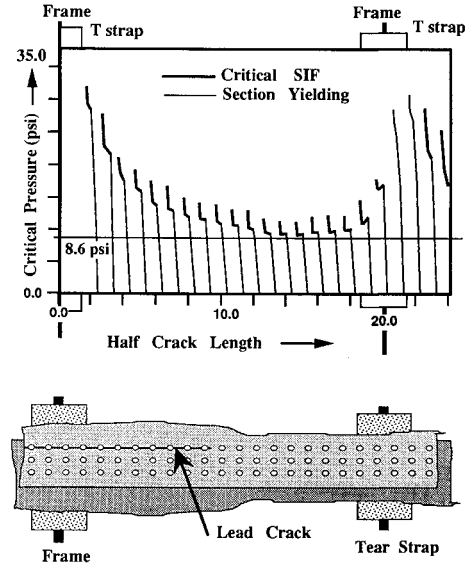


Fig. 5 Critical pressure diagram for a single dominant multibay crack at outer critical row of fastener holes in a lap splice.

and then local FEAM is applied to obtain crack tip SIF and the net section stresses.

In the last section we saw that the magnitude of crack length from the hole center (overhang) is an important factor in determining the critical pressure. For a single dominant crack, at the outer critical row of fasteners, spreading equally on both sides of a broken tear strap, the critical pressure diagram is shown in Fig. 5. Linkup stresses for the lead crack (ahead of which there are fastener holes, but without MSD cracks)

Table 2 Effect of MSD crack length on residual strength; set 2

Half lead-crack length	Critical internal pressure, psi							
	LEFM				Net section stress			
	MSD crack length			MSD crack length				
No MSD	0.12 in.	0.25 in.	0.35 in.	No MSD	0.12 in.	0.25 in.	0.35 in.	
1.75	29.0	28.2	28.1	27.9	39.4	38.5	30.2	23.0
3.75	19.4	19.0	18.8	18.5	28.6	27.5	21.4	16.2
5.75	14.9	14.8	14.6	14.3	22.3	21.3	16.6	12.5
7.75	12.4	12.5	12.4	12.1	18.5	17.7	13.8	10.4
9.75	11.0	11.2	11.1	10.9	16.1	15.4	12.0	9.1
11.75	10.1	10.3	10.2	10.1	14.5	13.9	10.8	8.2
13.75	9.4	9.7	9.7	9.5	13.5	12.9	10.0	7.7
15.75	9.1	9.6	9.6	9.4	13.0	12.4	9.7	7.4
17.75	9.8	10.1	10.1	10.0	13.7	13.3	10.4	8.0
18.75	11.6	12.2	12.1	12.1	16.1	15.6	12.3	9.6
19.75	16.8	18.5	18.5	18.4	21.1	20.7	16.5	13.0
20.75	28.0	31.7	31.9	32.1	24.5	24.3	19.6	15.6
21.75	26.1	27.9	27.9	27.9	26.7	26.1	20.8	16.3
22.75	22.1	22.8	22.6	22.4	25.7	25.0	19.8	15.3

correspond to the net section yield between the crack tip and the fastener hole. Up to about 40% overhang, the shell panel is  $K_c$  critical, and for the latter half, it has too little section strength. Interestingly, a two-bay crack is fully section strength critical. Frames/tear straps appear to provide adequate residual strength to the panel.

#### Single Dominant Crack and MSD at Fastener Holes

We now explore the effect of MSD near fastener holes ahead of the dominant crack in a lap splice. The important parameters are the lead crack length, the lead crack overhang from the nearest fastener hole, and the number and lengths of MSD cracks near fastener holes ahead of the lead crack. The MSD considered for the present purposes is over the three rivets immediately ahead of the lead crack tip, as the far-away MSD cracks have an insignificant effect on the lead crack tip stress field, and also have lower intact ligament stress.<sup>8</sup> In the MSD zone, cracks of equal length are presumed to be present on both sides of the rivet holes. To understand the MSD effects, for various lead crack lengths, starting from a situation where the lead crack spans over only two holes, to a situation of a multibay crack involving more than 40 rivets, the following two sets of crack configurations (overhang and MSD length) are analyzed: 1) MSD length of 0.12 in., which corresponds to the maximum that can hide under the countersunk head and stays undetected during regular economical nondestructive inspections. Two values of lead crack overhang, viz., 0.25 and 0.50 in., are considered; and 2) lead crack overhang of 0.25 in., and the MSD lengths of 0.12, 0.25, and 0.35 in.

The residual strengths for the two sets, computed based on linear elastic fracture mechanics and net section stress criteria, are presented in Tables 1 and 2.

From Table 1 it can be seen that the small MSD cracks (0.12 in.) have a marginal effect on the residual strength of the shell panel, whether it is computed based on fracture mechanics or section yielding criteria. Of course, for relatively large overhang values, e.g., 0.75 in., the section stress will shoot up with the presence of MSD.

As seen from Table 2, the effect of MSD crack length on the critical pressure, computed based on linear-elastic-fracture mechanics criterion, is marginal. The increase in MSD crack length has two effects:

1) It reduces the intact ligament length, raising the net section stresses and thus increasing the lead crack tip SIF.

2) It relieves the fastener load, diverting the sheet stresses away from the lead crack tip, reducing the lead crack tip SIF.

The net effect is the sum total of these two. For smaller MSD crack lengths, the load flow redistribution dominates

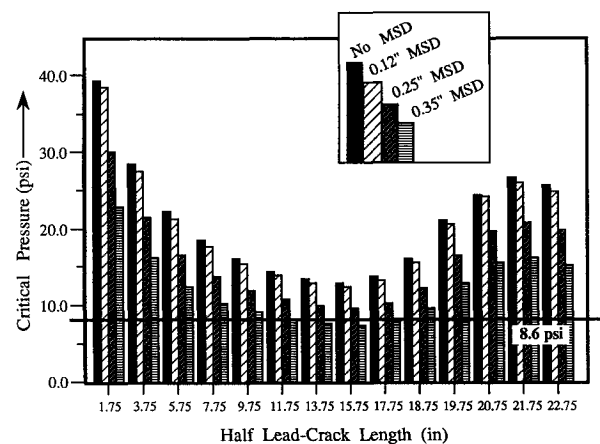


Fig. 6 Effect of MSD crack length on residual strength, based on net section yield criterion (see Table 2).

causing a fall in SIF. For longer MSD crack lengths, the net section overloading dominates and raises the SIF. But overall, the effect of MSD on lead crack tip SIF is marginal. However, the maximum net ligament stress increases steadily with increase in MSD lengths as the two crack tips come closer; in this case the plasticity dominates, and crack linkup based on the net section stress criterion is highly likely.

We see that the MSD does not significantly alter the lead crack tip SIF, but does raise the net ligament stress when the two crack tips come closer. The use of linear elastic fracture mechanics to study the effect of MSD infested holes ahead of a lead crack is thus questionable. It may be concluded that the effect of plasticity and net section yield dominate the situation when holes with MSD cracks are present ahead of a lead crack. The residual strength estimate, based on net section yield, is significantly reduced in the presence of MSD near holes ahead of a lead crack. Figure 6 represents the fall of residual strength with MSD crack length in the form of a bar chart. Also judging from the results in Sec. 5, it is the effect of holes ahead of the lead crack that is most dominant, whether or not these holes have MSD cracks emanating from them.

#### Elastic-Plastic Analysis of Flat Panels with MSD

Panels with the MSD cracks are analyzed using the elastic-plastic FEAM for critical strengths. An aluminum alloy (Al 2024-T3) sheet of width 20 in., height 40 in., and thickness 0.04 in., with a center crack of length  $2a$  and MSD cracks of length  $2b$  each is considered. Let the spacing between the

Table 3 Crack configurations<sup>a</sup>

Configuration	Lengths, in.			
	a	b	c	d
P1	2.00	—	—	—
P2	3.50	—	—	—
P3	5.25	—	—	—
P4	3.00	0.25	4.50	—
P5	3.60	0.25	4.50	—
P6	3.80	0.25	4.50	—

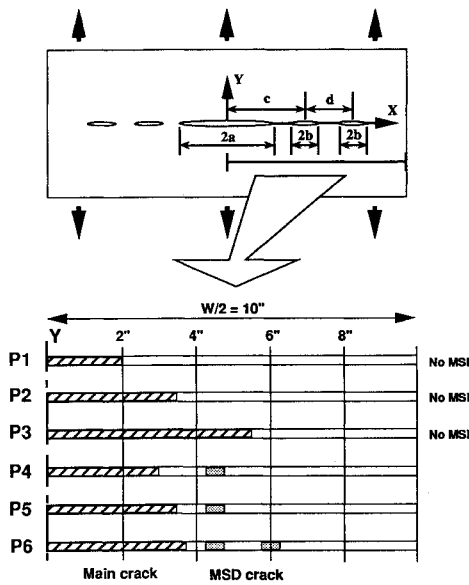
<sup>a</sup>See Fig. 7.

Fig. 7 Crack configurations of flat panels (see Table 3).

main crack and closest MSD crack be denoted by  $c$  and the MSD cracks be spaced apart by a distance  $d$ . The configuration, similar to those of experimental efforts at Foster Miller,<sup>14</sup> is shown in Fig. 7. Six configurations listed in Table 3 have been analyzed. The finite element mesh of the uncracked body (which is adequate for all crack configurations, in the present EP-FEAM) consists of 480 eight-noded isoparametric quadratic elements. Due to symmetry, only the upper half of the specimen is modeled.

### Results and Discussion

Either the  $T^*$  integral or the crack tip opening angle (CTOA) can be used as a fracture criterion for the stable crack growth simulation. Both the  $T^*$  integral and CTOA remain constant during elastic-plastic stable crack growth.<sup>9</sup> We employ  $T^*$  integral as the crack tip parameter, whose critical value governs the crack propagation. In order to find the critical  $T^*$  value, single crack cases (P1, P2, and P3) are analyzed and compared with the experimental results as shown in Fig. 8. Two critical values for the initiation and the saturation are evaluated as 200 and 710 lb/in., respectively. Based on these  $T^*$  values, the residual strengths for panels P4, P5, and P6 evaluated using EP-FEAM, are shown in Figs. 9–11. It can be seen from these figures that the computed results agree well with the experimental ones. We observe from panels P2 and P5, which have almost the same main crack length, the far-field critical stress with MSD crack (P5) is about 20% lower as compared to the one without MSD (P2). Thus, even small MSD crack can significantly reduce the residual strength of the panel.

CTOA is a parameter defined from the deformation of the material just behind the current crack tip.<sup>15</sup> The evaluation of CTOA using a conventional finite element method requires a very fine mesh discretization. On the other hand, the  $T^*$

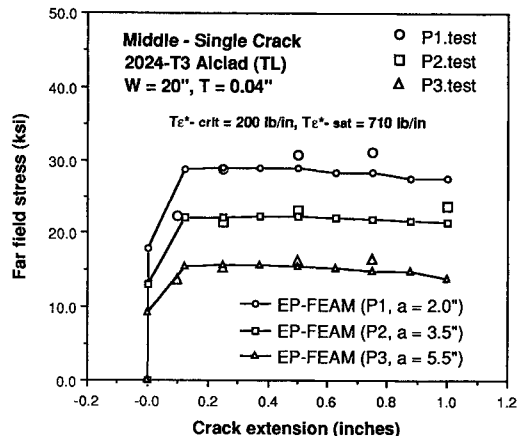


Fig. 8 Comparison of tested and evaluated results for specimens P1, P2, and P3.

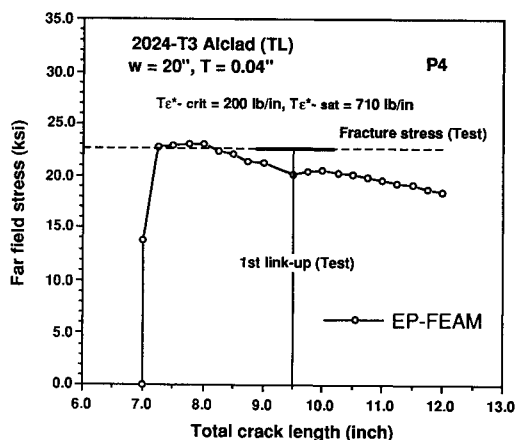


Fig. 9 Comparison of tested and predicted results for specimen P4.

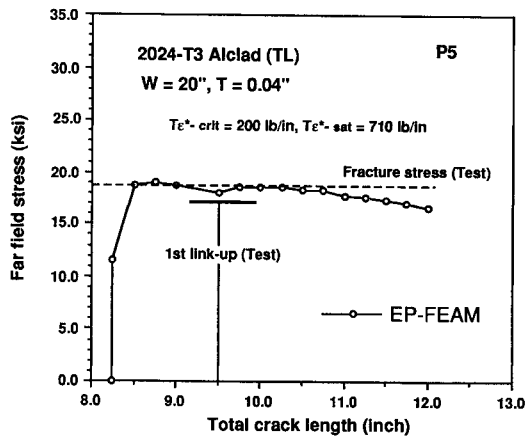


Fig. 10 Comparison of tested and predicted results for specimen P5.

integral is calculated as an integral over the domain between the far-field contour and a contour in close vicinity of the crack tip (i.e., equivalent domain integral method<sup>10</sup>). Unlike the CTOA, which is a highly localized deformation parameter, the  $T^*$  is an averaged parameter of deformation field over the integration area. Its evaluation does not strongly depend on the deformation field in a small region around the crack tip, rather it relies on the overall deformation field of cracked body. This feature dispenses the need for a fine mesh. For example, the problem, which was analyzed by Newman et al.<sup>15</sup> using 6500 nodes to get a reasonable value of CTOA, the present analysis using EP-FEAM needs as low as 1559 nodes to get  $T^*$ , bringing down the CPU time by an order

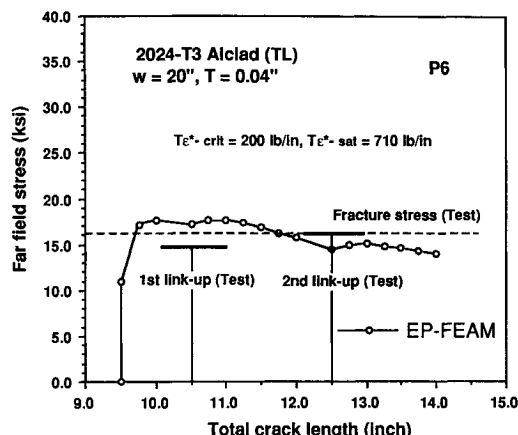


Fig. 11 Comparison of tested and predicted results for specimens P6.

of 50. Another advantage of FEAM is that the crack tip position can be set regardless of the finite element mesh. This allows the incremental crack extension length in the crack propagation analysis to be independent of the mesh. A conventional FE approach needs a row of extremely fine mesh discretization along the line of crack propagation with the incremental crack length of at least one element size.

These two factors make the application of elastic-plastic finite element alternating method with  $T^*$  as the fracture criterion, a very efficient tool to study the MSD link-up phenomenon.

### Conclusions

The global FEM and local FEAM elastic analyses of the fuselage stiffened shell panels, with longitudinal cracks at various locations, shows that the presence of rivet holes (with or without MSD emanating from these holes) ahead of a lead crack significantly reduces the residual strength of the damaged panel computed based on the section yielding criterion. The most important parameter turns out to be the location of the lead crack tip with respect to the holes and MSD crack tips. If the net ligament is small the section stresses shoot up, bringing the residual strength to a very low value. This brings out the need for complete elastic-plastic analysis. The EP-FEAM, with  $T^*$  as the fracture criterion for stable crack growth, could be successfully applied to the problems of MSD in flat panels.

### Acknowledgments

The authors are grateful for the financial support from the Federal Aviation Administration to the Center of Excellence for Computational Modeling of Aircraft Structures, Georgia

Institute of Technology, Atlanta, Georgia. They also acknowledge with pleasure the discussions and support from various colleagues, in particular Tom Swift and Paul Tan of the FAA.

### References

- 1Park, J. H., and Atluri, S. N., "Fatigue Growth of Multiple Cracks near a Row of Fastener Holes in a Fuselage Lap Joint," *Proceedings of the International Workshop on Structural Integrity of Aging Airplanes*, edited by Atluri et al., Atlanta, GA, 1992, pp. 91-116; also *Computational Mechanics*, Vol. 13, 1993, pp. 189-203.
- 2Nikishkov, G. P., and Atluri, S. N., "An Analytical-Numerical Alternating Method of Elastic-Plastic Analysis of Cracks," *Computational Mechanics*, Vol. 13, pp. 427-442.
- 3Ashwell, D. G., and Sabir, A. B., "A New Cylindrical Shell Finite Element Based on Simple Independent Shape Functions," *International Journal of Mechanical Sciences*, Vol. 14, 1972, pp. 171-183.
- 4Swift, T., "Fracture Analysis of Stiffened Structures," American Society of Testing and Materials, ASTM STP 842, 1984, pp 69-107.
- 5Park, J. H., Ogiso, T., and Atluri, S. N., "Analysis of Cracks in Aging Aircraft Structures, with and Without Composite Patch Repairs," *Computational Mechanics*, Vol. 10, Nos. 3/4, 1992, pp. 169-202.
- 6Shenoy, V. B., Potyondy, D. O., Atluri, S. N., "A Methodology for Computing Non-linear Fracture Parameters for a Bulging Crack in a Pressurised Aircraft Fuselage," *Computational Mechanics* (to be published).
- 7Nayak, G. C., and Zienkiewicz, O. C., "Elasto-Plastic Stress Analysis. A Generalization for Various Constitutive Relations Including Strain Softening," *International Journal of Numerical Methods in Engineering*, Vol. 5, 1972, pp. 113-135.
- 8Park, J. H., Ripudaman, S., Pyo, C. R., and Atluri, S. N., "Structural Integrity of Panels with Multi-Site Damage," *Proceedings of the AIAA/ASME/ASCE/AHS/ACS 35th SDM Conference* (Hilton Head, SC), 1994, pp. 1191-1200 (AIAA Paper 94-1457).
- 9Atluri, S. N., "Energetic Approaches and Path-Independent Integrals in Fracture Mechanics," *Computational Methods in the Mechanics of Fracture*, edited by S. N. Atluri, Elsevier, 1986, pp. 121-165.
- 10Nikishkov, G. P., and Atluri, S. N., "An Equivalent Domain Integral Method for Computing Crack Tip Integral Parameters in Non-Elastic, Thermo-Mechanical Fracture," *Engineering Fracture Mechanics*, Vol. 26, 1987, pp. 851-867.
- 11Swift, T., "Damage Tolerance in Pressurized Fuselages," 11th Plantema Memorial Lecture, ICAF, Canada, 1987.
- 12Swift, T., "Residual Strength of Stiffened Structures," Lecture at Georgia Inst. of Technology, Atlanta, GA, Feb. 10, 1993.
- 13Jones, R., private communication, Monash Univ., Australia, Jan. 1993.
- 14Jeong, D. Y., "Preliminary Analysis of FMI Flat Panel Experiments," Foster-Miller and Teledyne Engineering Services, Draft Rept., Dec. 1992.
- 15Newman, J. C., Jr., Dawicke, D. S., Sutton, M. A., and Bigelow, C. A., "A Fracture Criterion for Wide-Spread Cracking in Thin Sheet Aluminium Alloys," ICAF, Stockholm, Sweden, 1993.